eLIFE elifesciences.org

RESEARCH ARTICLE

Figures and figure supplements

Maternally provided LSD1/KDM1A enables the maternal-to-zygotic transition and prevents defects that manifest postnatally

Jadiel A Wasson *et al*

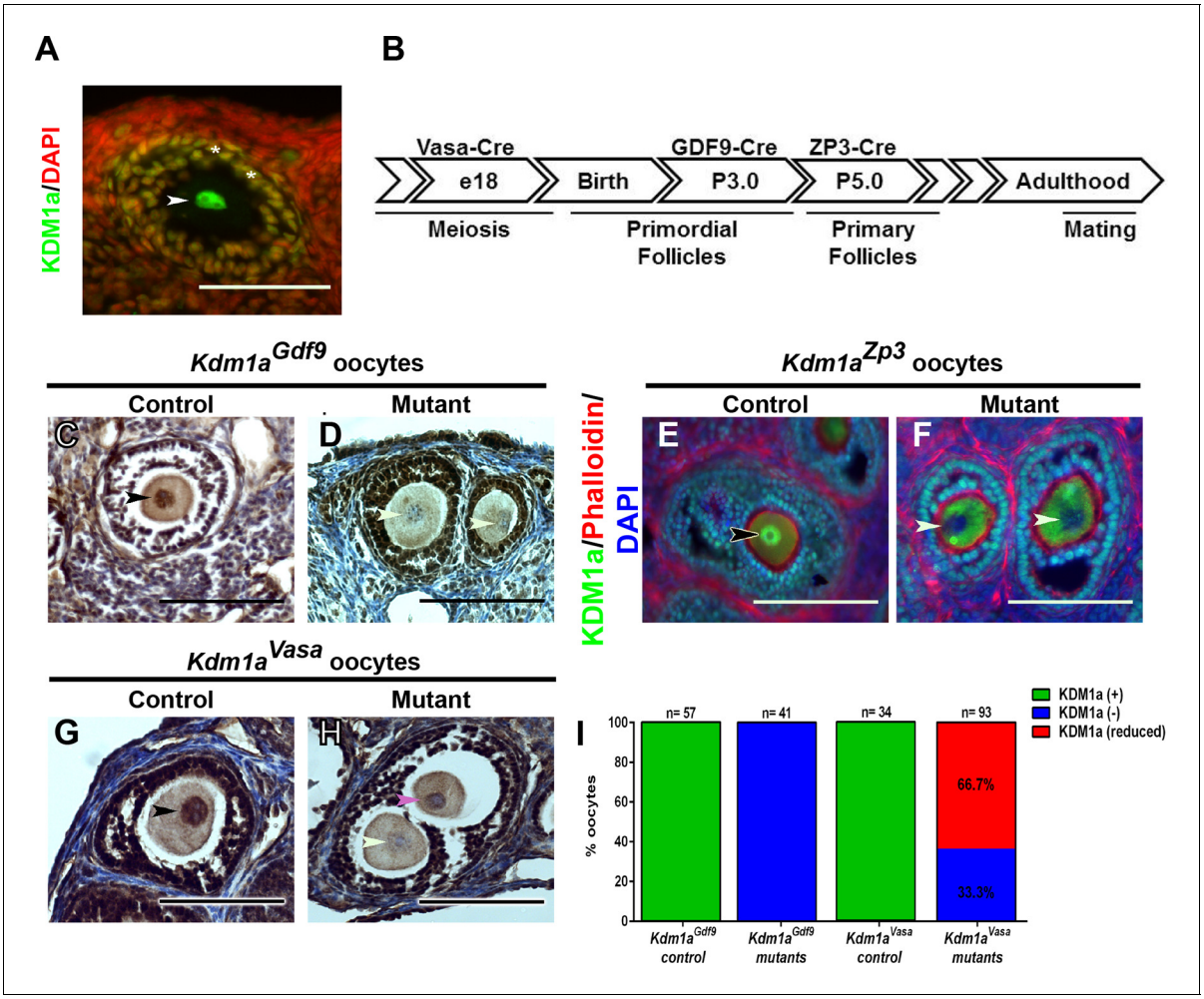

Figure 1. Maternal expression and coditional deletion of *Kdm1a* in mouse oocytes. (**A**) Wild-type mouse oocyte nucleus (white arrowhead) and surrounding follicle cells (white asterisks) stained with anti-KDM1A (green) antibody and DAPI (red). (**B**) Developmental timeline of maternal *Cre* expression (*Vasa-Cre, Gdf9-Cre* and *Zp3-Cre* transgenes) and corresponding oogenesis stages. (**C**,**D**) Immunohistochemistry (IHC) with anti-KDM1A (brown) antibody and hematoxylin (blue) showing KDM1A nuclear expression (black arrowhead) and absence of expression (white arrowheads) in $Kdm1a^{Gdf9}$ control (**C**) and mutant (**D**) oocytes. (**E**,**F**) Immunofluorescence (IF) with anti-KDM1A (green) antibody, phalloidin (red) and DAPI (blue) showing KDM1A nuclear expression (black arrowhead) and absence of expression (white arrowheads) in $Kdm1a^{Zp3}$ control (**E**) and mutant (**F**) oocytes. (**G**,**H**) IHC with anti-KDM1A (brown) antibody and hematoxylin (blue) showing KDM1A nuclear expression (black arrowhead), absence of expression (white arrowhead) and reduced expression (pink arrowhead) in $Kdm1a^{Vasa}$ control (**G**) and mutant (**H**) oocytes. (**I**) Percentage of oocytes with KDM1A (green), reduced KDM1A (red) or no KDM1A blue) staining in $Kdm1a^{Gdf9}$ and $Kdm1a^{Vasa}$ heterozygous control versus mutant oocytes. Scale bars represent 50 μm. n=number of oocytes analyzed with percentages indicated for each category.

DOI: 10.7554/eLife.08848.003

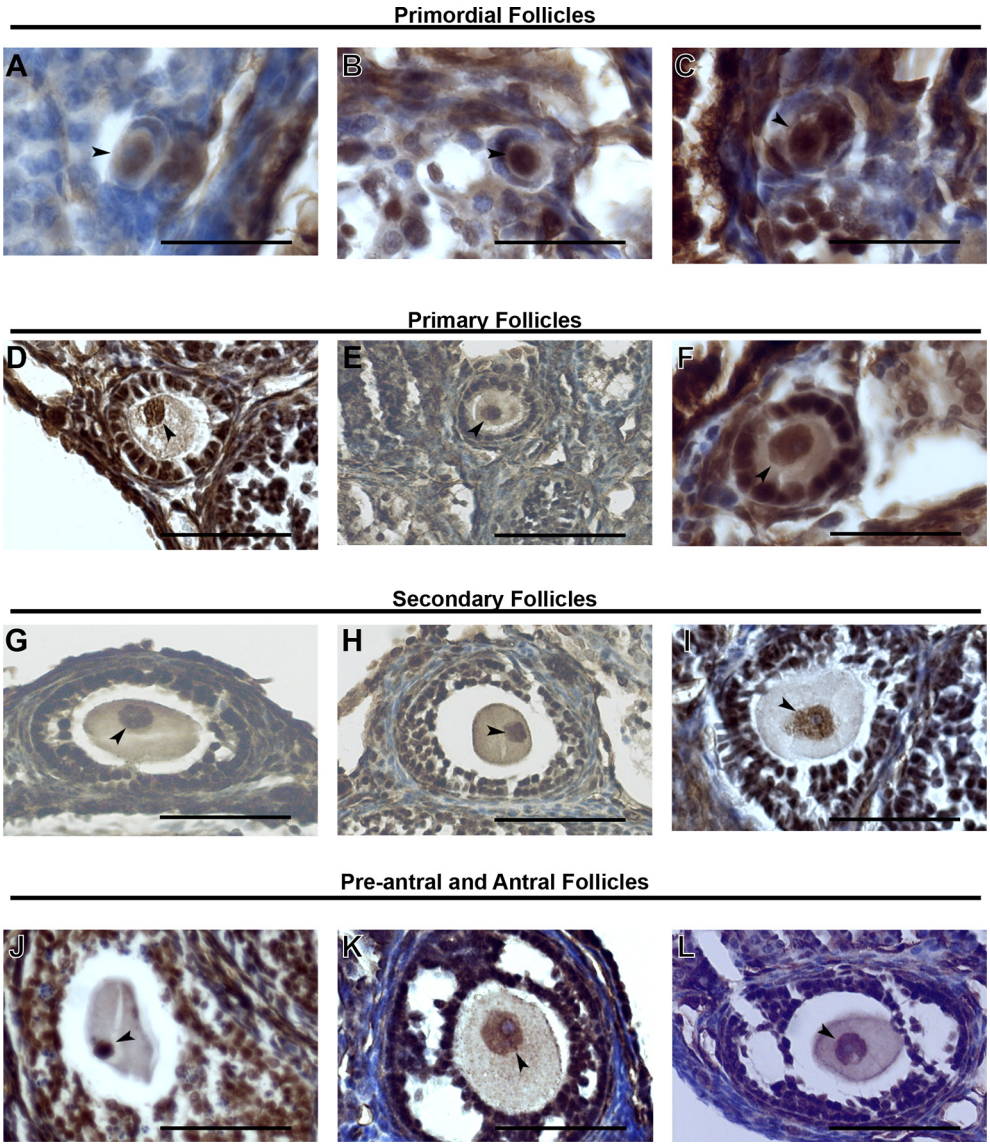

Figure 1—figure supplement 1. KDM1A expression in stged oocytes. (**A–L**) Immunohistochemistry (IHC) of primordial follicles (**A–C**), primary follicles (**D–F**), secondary follicles (**G-I**) and pre-antral and antral follicles (**J–L**) stained with anti-KDM1A(brown) antibody and hematoxylin (blue). The oocyte nucleus is indicated with black arrowheads. Scale bars represent 50 μm.

DOI: 10.7554/eLife.08848.004

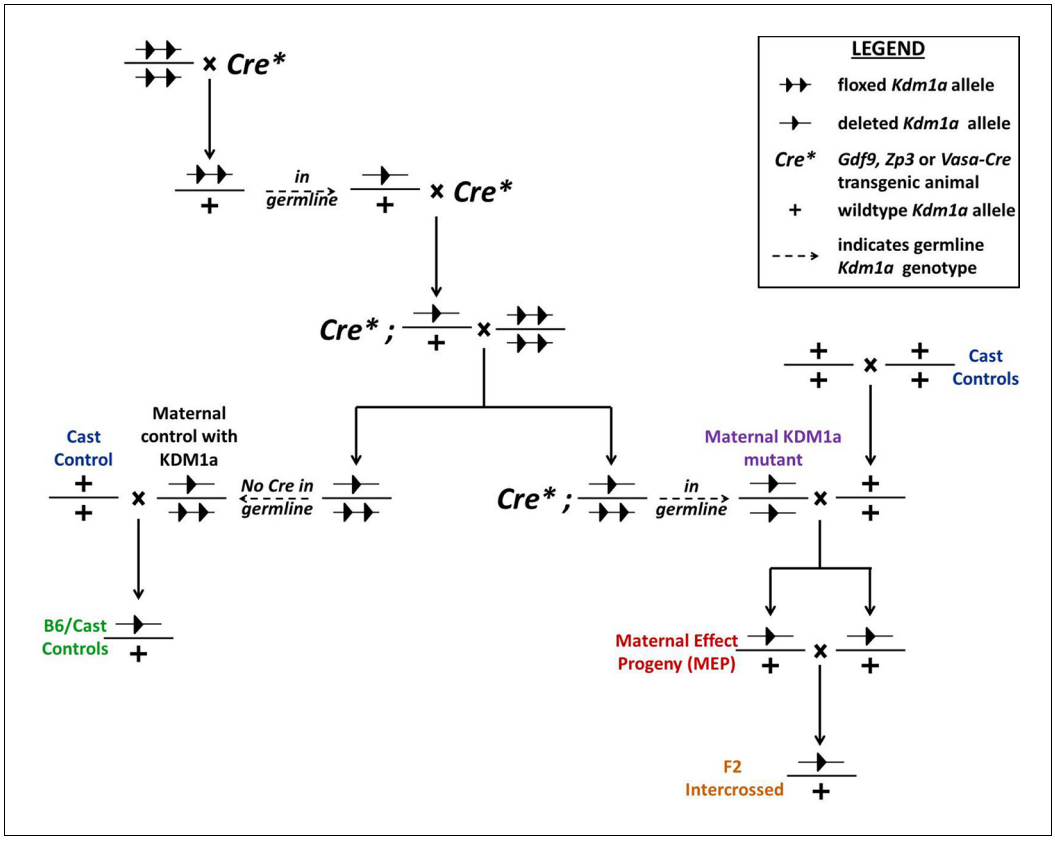

Figure 1—figure supplement 2. Generation of *Kdm1a* mutant and control animals. *Kdm1a* animals were generated by crossing multiple generations of *Kdm1a*$^{fl/fl}$ animals with either *Gdf9-*, *Zp3-*, or *Vasa-Cre* transgenic animals. Blue indicates *Mus castaneus* control animals. Purple indicates *Kdm1a* mutant females. Green indicates B6/Cast hybrid control progeny. Red indicates *Kdm1a* maternal effect progeny (MEP). Orange indicates progeny resulting from intercrossing 2 MEP adult animals. All labelled progeny were used in crosses and assays presented in subsequent figures (color-coding matches animals used and graphed in each figure).
DOI: 10.7554/eLife.08848.005

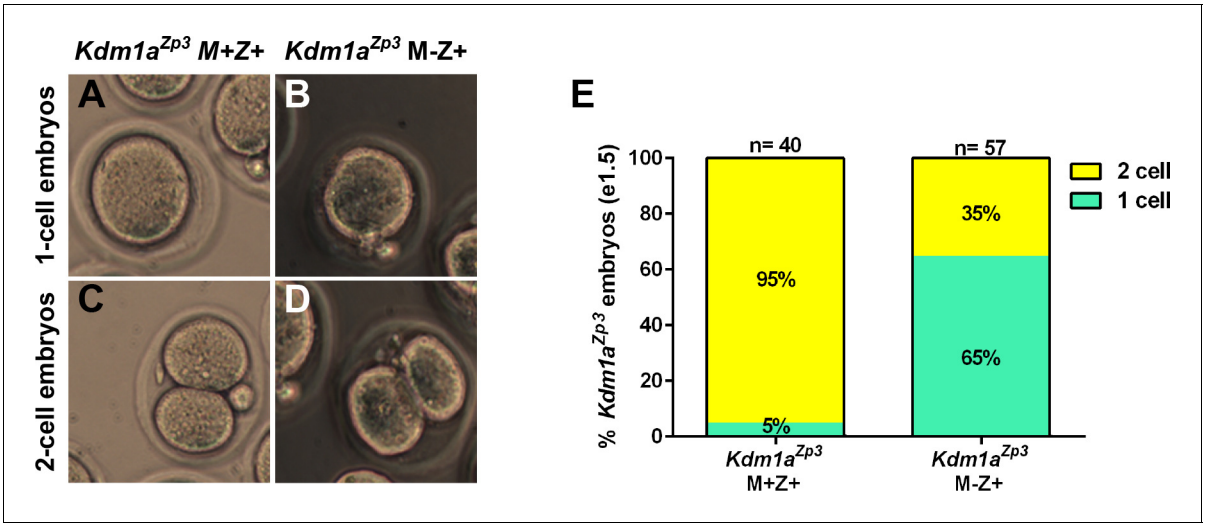

Figure 2. *Kdm1a*^{Zp3} embryos arrest at the 1–2 cell stage. (**A–D**) Brightfield images of (**A**,**C**) M+Z+ and (**B**,**D**) M-Z+ 1- and 2-cell embryos derived from *Kdm1a*^{Zp3} control and mutant mothers at e1.5. (**E**) Percentage of 1-cell (green) and 2-cell (yellow) embryos derived from *Kdm1a*^{Zp3} control and mutant mothers at e1.5. n = 40 for *Kdm1a*^{Zp3} M+Z+ embryos from 3 litters. n = 57 for *Kdm1a*^{Zp3} M-Z+ embryos from 6 litters.
DOI: 10.7554/eLife.08848.006

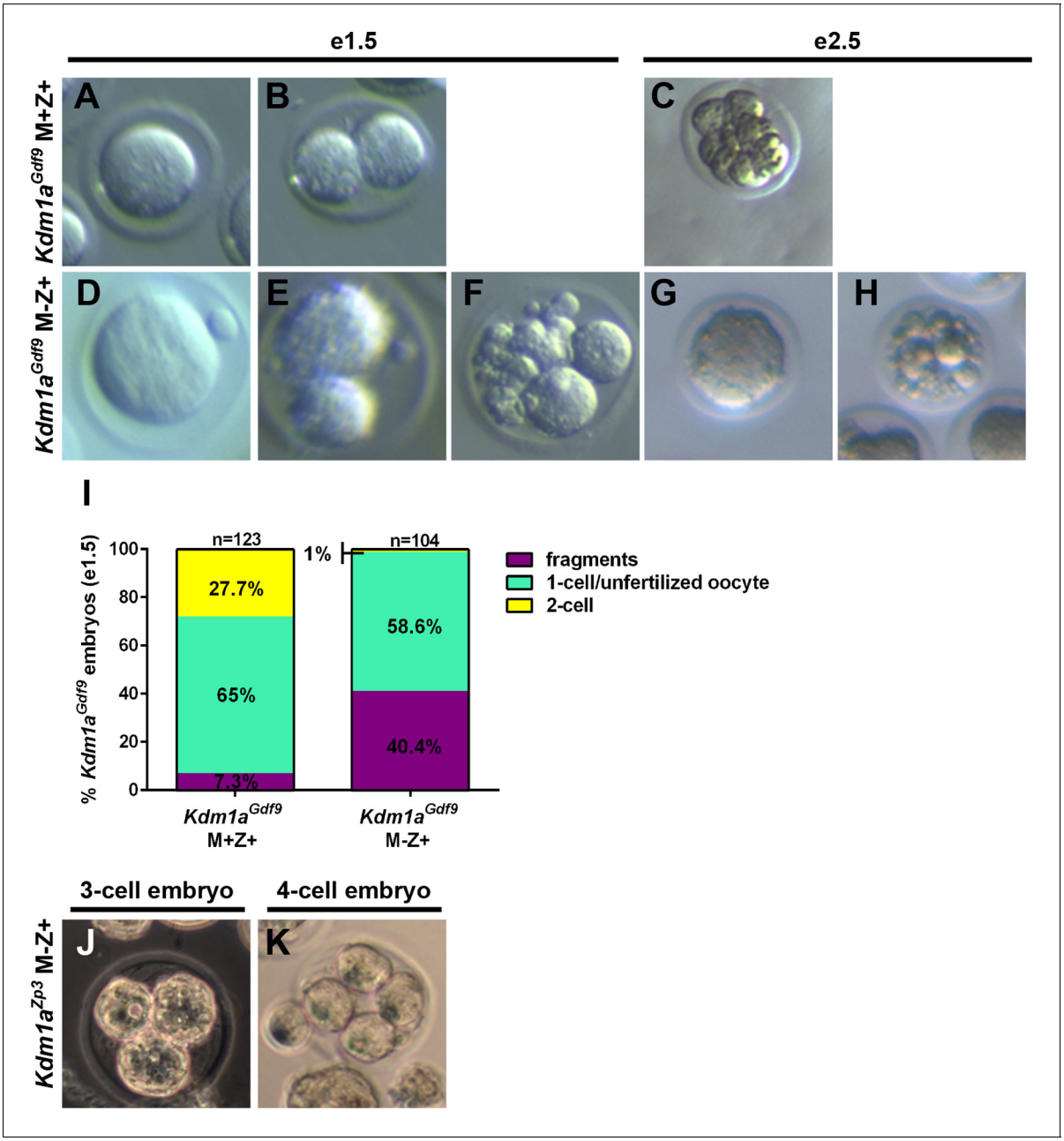

Figure 2—figure supplement 1. Lack of normal *Kdm1a*^{Gdf9} and *Kdm1a*^{Zp3} embryos at embryonic day 1.5 and 2.5. (**A**,**B**,**D**,**E**,**F**) Brightfield images of embryonic day 1.5 (e1.5) M+Z+ 1-cell (**A**) and 2-cell (**B**) embryos and M-Z+ 1-cell (**D**), 2-cell (**E**), and fragmented (**F**) embryos derived from *Kdm1a*^{Gdf9} control and mutant mothers. (**C**,**G**,**H**) Brightfield images of e2.5 M+Z+ 8-cell (**C**) embryo and M-Z+ abnormal 1-cell (**G**), and fragmented (**H**) embryos derived from *Kdm1a*^{Gdf9} control and mutant mothers. (**I**) Percentage of fragmented (purple), unfertilized oocyte or 1C (green), and 2C (yellow) embryos from *Kdm1a*^{Gdf9} control and mutant mothers. n = 123 for *Kdm1a*^{Gdf9} M+Z+ control embryos from 8 litters. n = 104 for *Kdm1a*^{Gdf9} M-Z+ embryos from 8 litters. (**J**) Brightfield image of 3-cell M-Z+ embryo derived from a *Kdm1a*^{Zp3} mutant mother. (**K**) Brightfield image of 4-cell M-Z+ embryo derived from a *Kdm1a*^{Zp3} mutant mother.

DOI: 10.7554/eLife.08848.007

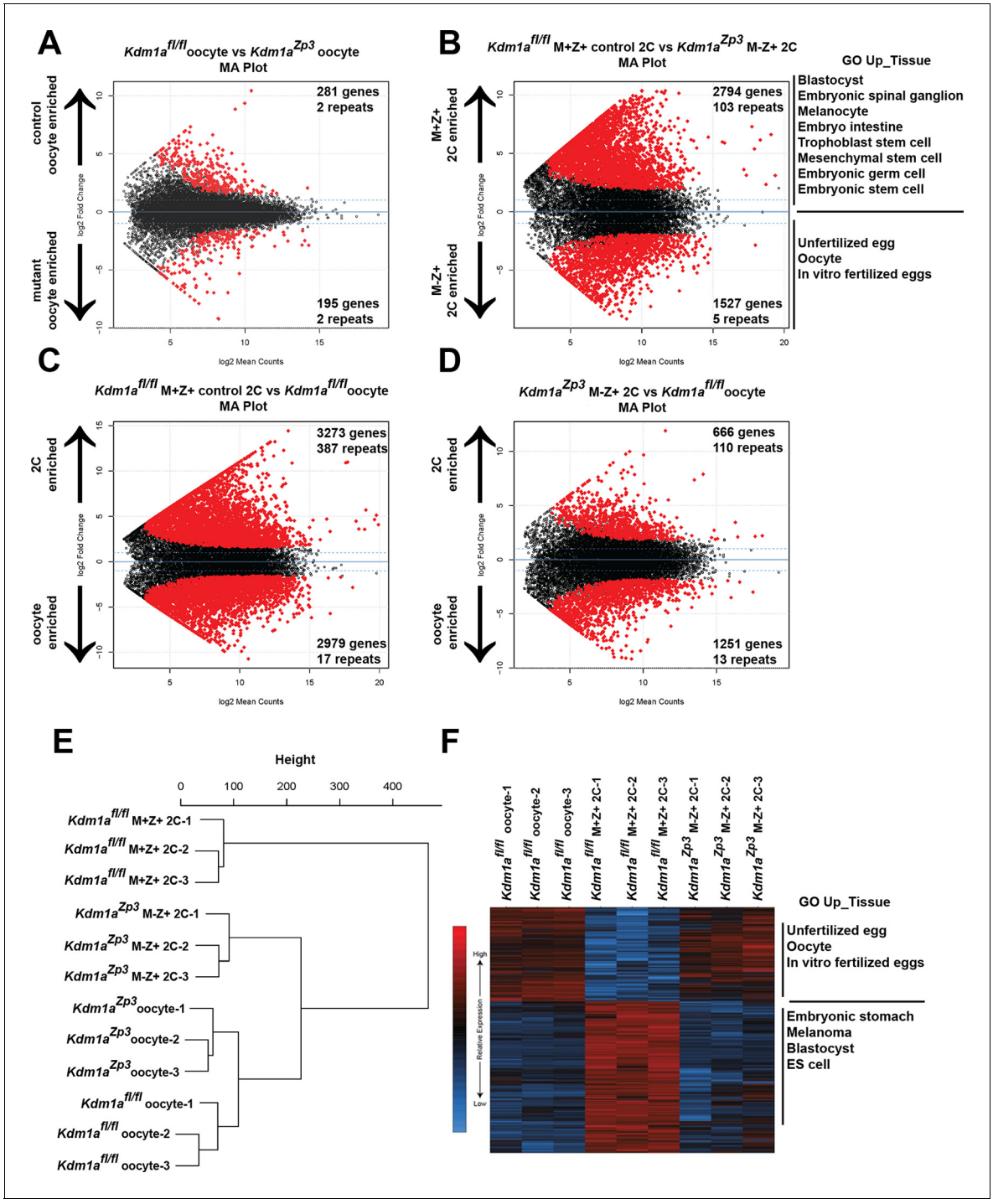

Figure 3. The MZT is impaired in *Kdm1a*^{Zp3} mutants. (**A**,**B**) Differential expression of mRNAs in *Kdm1a*$^{fl/fl}$ versus *Kdm1a*^{Zp3} oocytes (**A**) or *Kdm1a*$^{fl/fl}$ M+Z+ versus *Kdm1a*^{Zp3} M-Z+ 2C embryos (**B**) as determined by RNA-seq. Genes/repeats highlighted in red are significant with the number of significant gene/repeats show. GO enrichment using the Up_tissue database was performed on *Kdm1a*$^{fl/fl}$ M+Z+ 2C enriched and *Kdm1a*^{Zp3} M-Z+ 2C enriched mRNAs, with a list of the most enriched categories displayed. (**C**,**D**) Differential expression of mRNAs in *Kdm1a*$^{fl/fl}$ M+Z+ 2C embryos versus *Kdm1a*$^{fl/fl}$ oocytes (**C**) or *Kdm1a*^{Zp3} M-Z+ 2C embryos versus *Kdm1a*$^{fl/fl}$ oocytes (**D**). The numbers of zygotically activated (2C enriched) genes/repeats and zygotically repressed (oocyte enriched) genes/repeats are highlighted in each comparison. (**E**) Hierarchical cluster dendrogram of transcriptomes in *Kdm1a*$^{fl/fl}$ oocytes, *Kdm1a*^{Zp3} oocytes, *Kdm1a*$^{fl/fl}$ M+Z+ 2C embryos, and *Kdm1a*^{Zp3} M-Z+ 2C embryos. (**F**) Heat map of gene expression of principal component 1 (PC1) genes in *Kdm1a*$^{fl/fl}$ oocytes, *Kdm1a*$^{fl/fl}$ M+Z+ 2C embryos, and *Kdm1a*^{Zp3} M-Z+ 2C embryos. The most GO Up_tissue enriched terms are displayed for the 2 categories of PC1 genes.

DOI: 10.7554/eLife.08848.008

Figure 3 continued on next page

Figure 3 continued

The following source data is available for figure 3:

Source data 1. Gene Table comparison of *Kdm1a*$^{fl/fl}$ oocytes and *Kdm1a*^{Zp3} oocytes.
DOI: 10.7554/eLife.08848.009
Source data 2. Gene Table comparison of *Kdm1a*^{Zp3} M+Z+ 2C and *Kdm1a*^{Zp3} M-Z+ 2C embryos.
DOI: 10.7554/eLife.08848.010
Source data 3. Gene Table comparison of *Kdm1a*^{Zp3} M+Z+ 2C and *Kdm1a*$^{fl/fl}$ oocytes.
DOI: 10.7554/eLife.08848.011
Source data 4. Gene Table comparison of *Kdm1a*^{Zp3} M-Z+ 2C and *Kdm1a*$^{fl/fl}$ oocytes.
DOI: 10.7554/eLife.08848.012

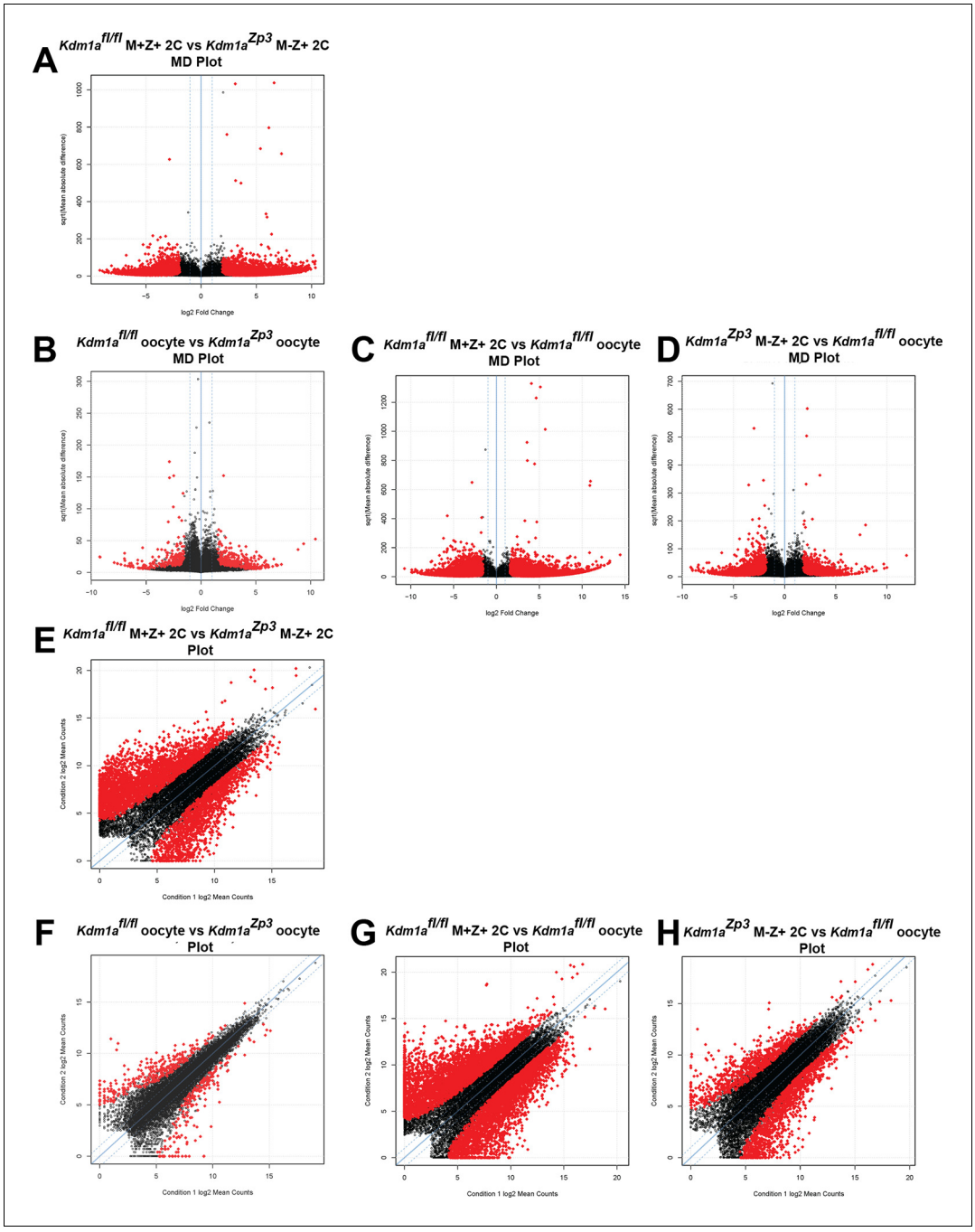

Figure 3—figure supplement 1. The MZT is impaired in *Kdm1a*^{Zp3} mutants. (**A–H**) Differential expression of mRNAs in *Kdm1a*$^{fl/fl}$ versus *Kdm1a*^{Zp3} oocytes (**A**,**E**), *Kdm1a*$^{fl/fl}$ M+Z+ versus *Kdm1a*^{Zp3} M-Z+ 2C embryos (**B**,**F**), *Kdm1a*$^{fl/fl}$ M+Z+ 2C embryos versus *Kdm1a*$^{fl/fl}$ oocytes (**C**,**G**), and *Kdm1a*^{Zp3} M-Z+ 2C embryos versus *Kdm1a*$^{fl/fl}$ oocytes (**D**,**H**) as determined by RNA-seq. Differential expression represented in mean difference plots (**A–D**) and normalized FPKM values on XY scatter plots (**E–H**). Genes/repeats highlighted in red are significant.
DOI: 10.7554/eLife.08848.013

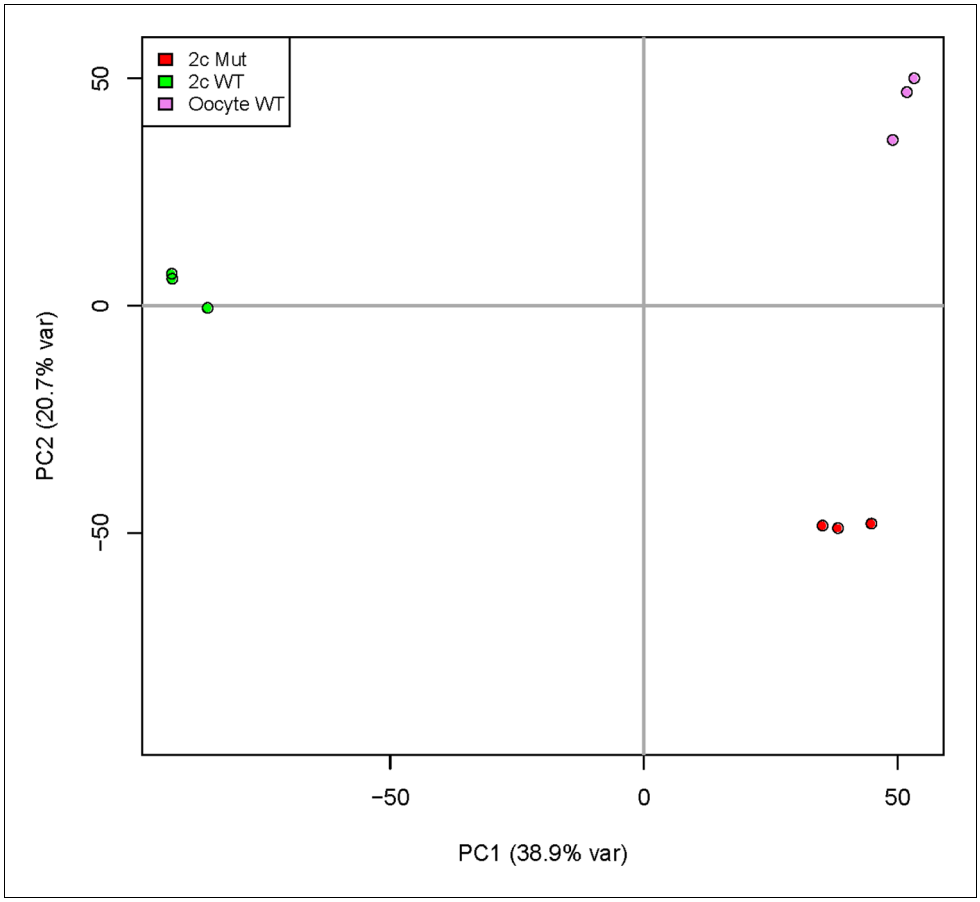

Figure 3—figure supplement 2. Principal component analysis of *Kdm1a*^{Zp3} 2C embryos. (**A**) Principal Component 1 is plotted on x-axis and Principal Component 2 is plotted on y-axis. Variance due to each component for *Kdm1a*^{Zp3} M-Z+ 2C embryos (red), *Kdm1a*$^{fl/fl}$ M+Z+ 2C embryos (green), and *Kdm1a*$^{fl/fl}$ oocytes (purple) are shown.

DOI: 10.7554/eLife.08848.014

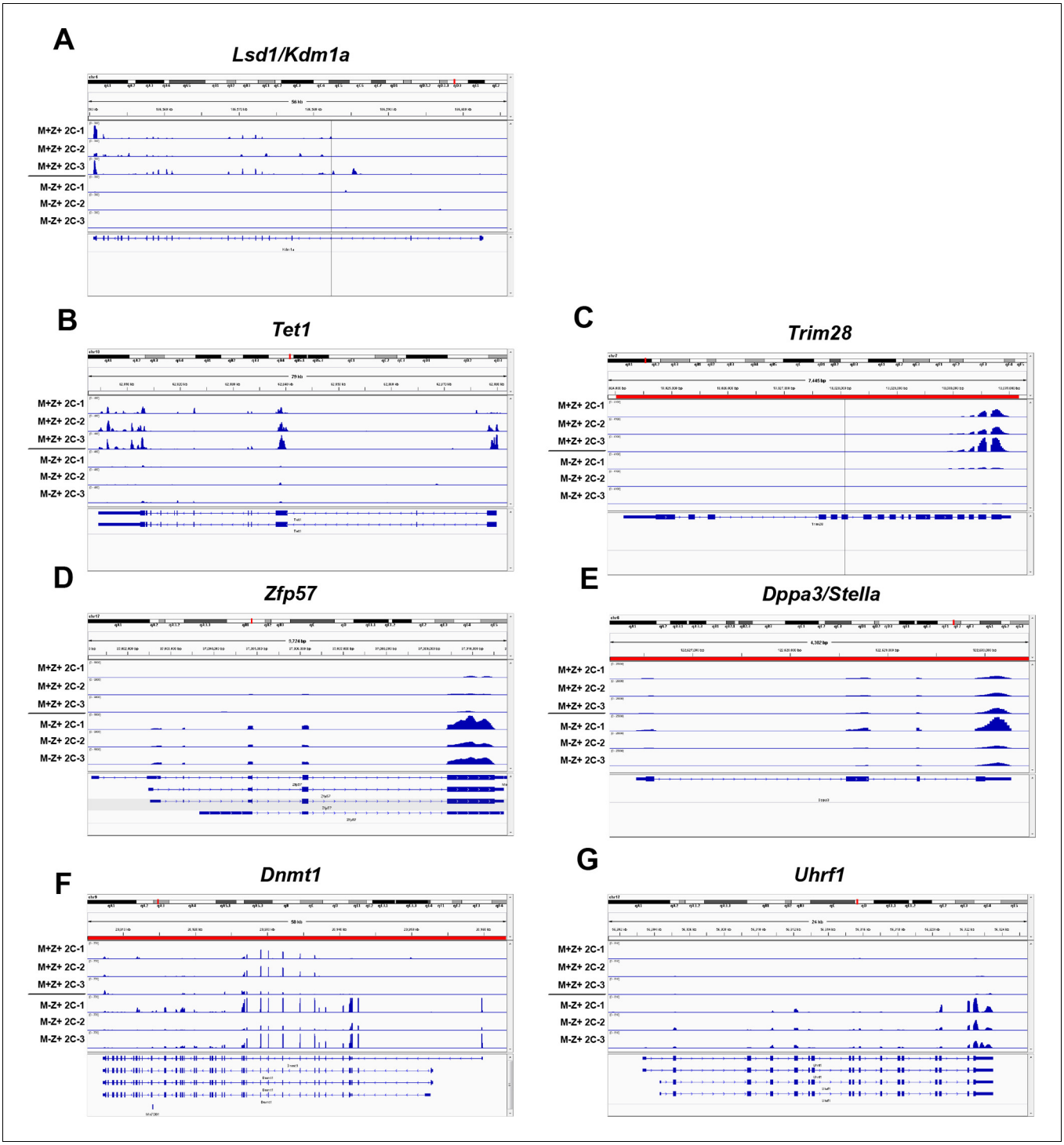

Figure 3—figure supplement 3. Expression of epigenetic regulators in *Kdm1a*^{Zp3} 2C embryos. Sequenced RNA-seq reads showing relative expression from *Kdm1a*$^{fl/fl}$ M+Z+ 2C embryos and *Kdm1a*^{Zp3} M-Z+ 2C embryos aligned to the genome for *Lsd1/Kdm1a* (**A**), *Tet1* (**B**), *Trim28* (**C**), *Zfp57* (**D**), *Dppa3/stella* (**E**), *Dnmt1* (**F**) and *Uhrf1* (**G**). Gene tracks visualized using Integrative Genomics Viewer.

DOI: 10.7554/eLife.08848.015

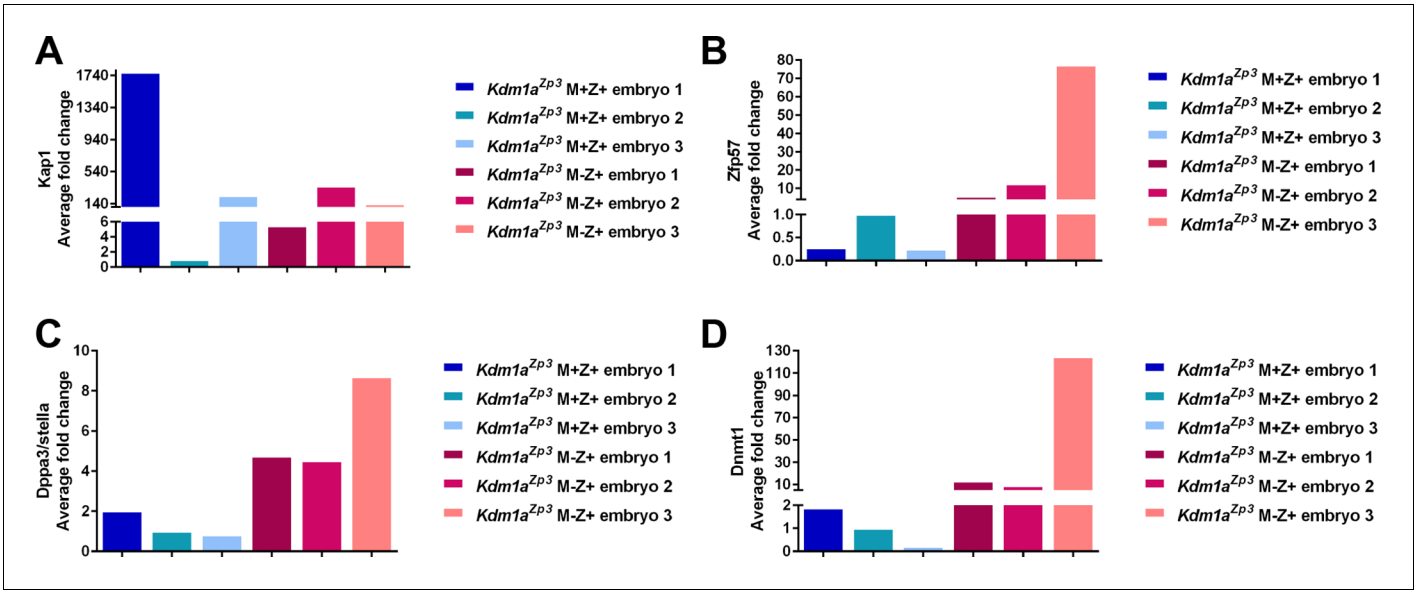

Figure 3—figure supplement 4. Relative expression of epigenetic regulators in *Kdm1a*^{Zp3} 2C embryos. Quantitative RT-PCR analysis of epigenetic regulators including *Trim28* (**A**), *Zfp57* (**B**) *Dppa3/stella* (**C**), and *Dnmt1* (**D**) in *Kdm1a*^{Zp3} M+Z+ 2C embryos compared to *Kdm1a*^{Zp3} M-Z+ 2C embryos. Y-axis represents average fold change. All gene expression was normalized to *Hprt* expression.

DOI: 10.7554/eLife.08848.016

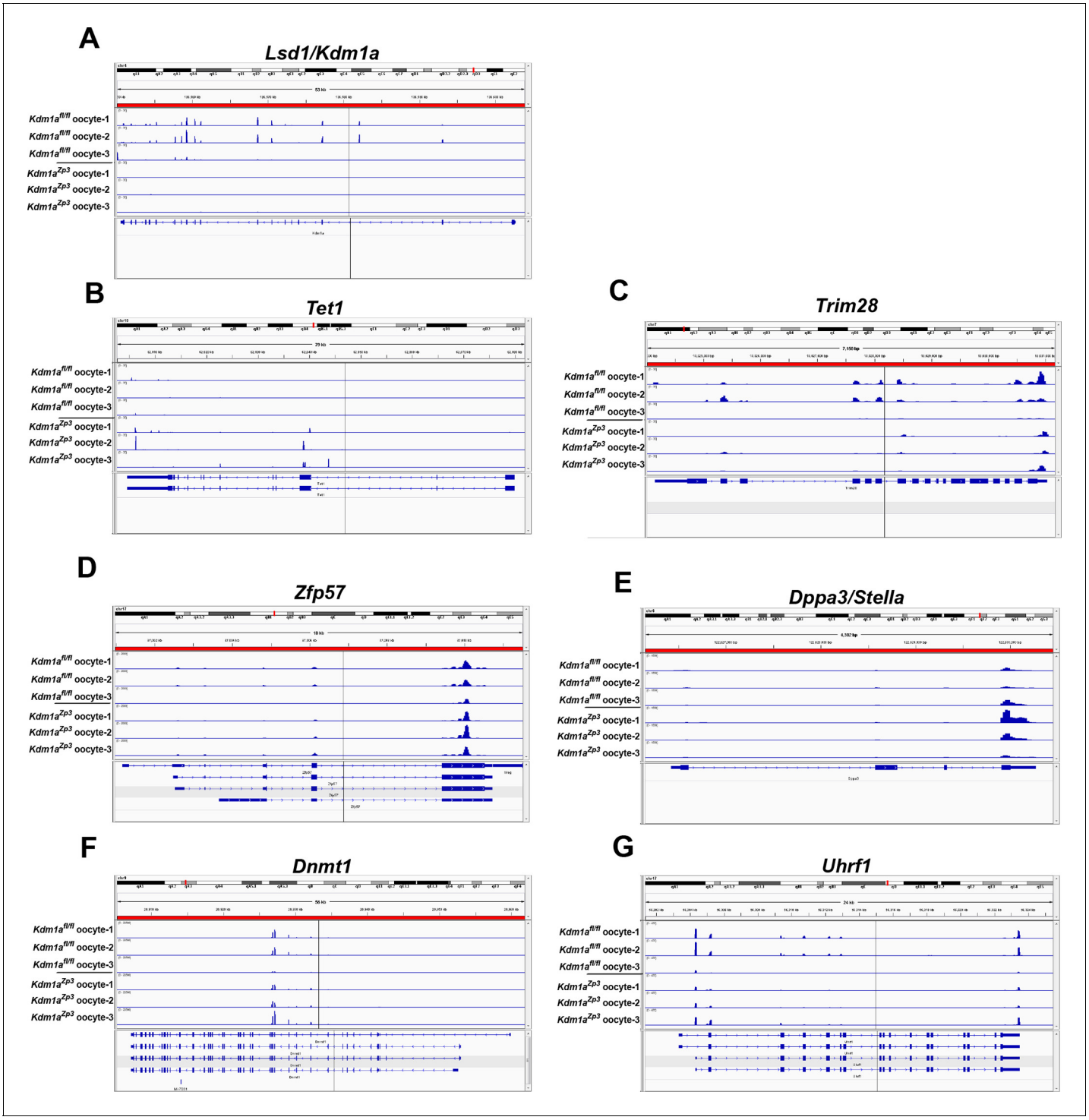

Figure 3—figure supplement 5. Expression of epigenetic regulators in *Kdm1a*$^{fl/fl}$ and *Kdm1a*^{Zp3} oocytes. Sequenced RNA-seq reads showing relative expression from *Kdm1a*$^{fl/fl}$ oocytes and *Kdm1a*^{Zp3} mutant oocytes aligned to the genome for *Lsd1/Kdm1a* (**A**), *Tet1* (**B**), *Trim28* (**C**), *Zfp57* (**D**), *Dppa3/stella* (**E**), *Dnmt1* (**F**) and *Uhrf1* (**G**). Gene tracks visualized using Integrative Genomics Viewer.

DOI: 10.7554/eLife.08848.017

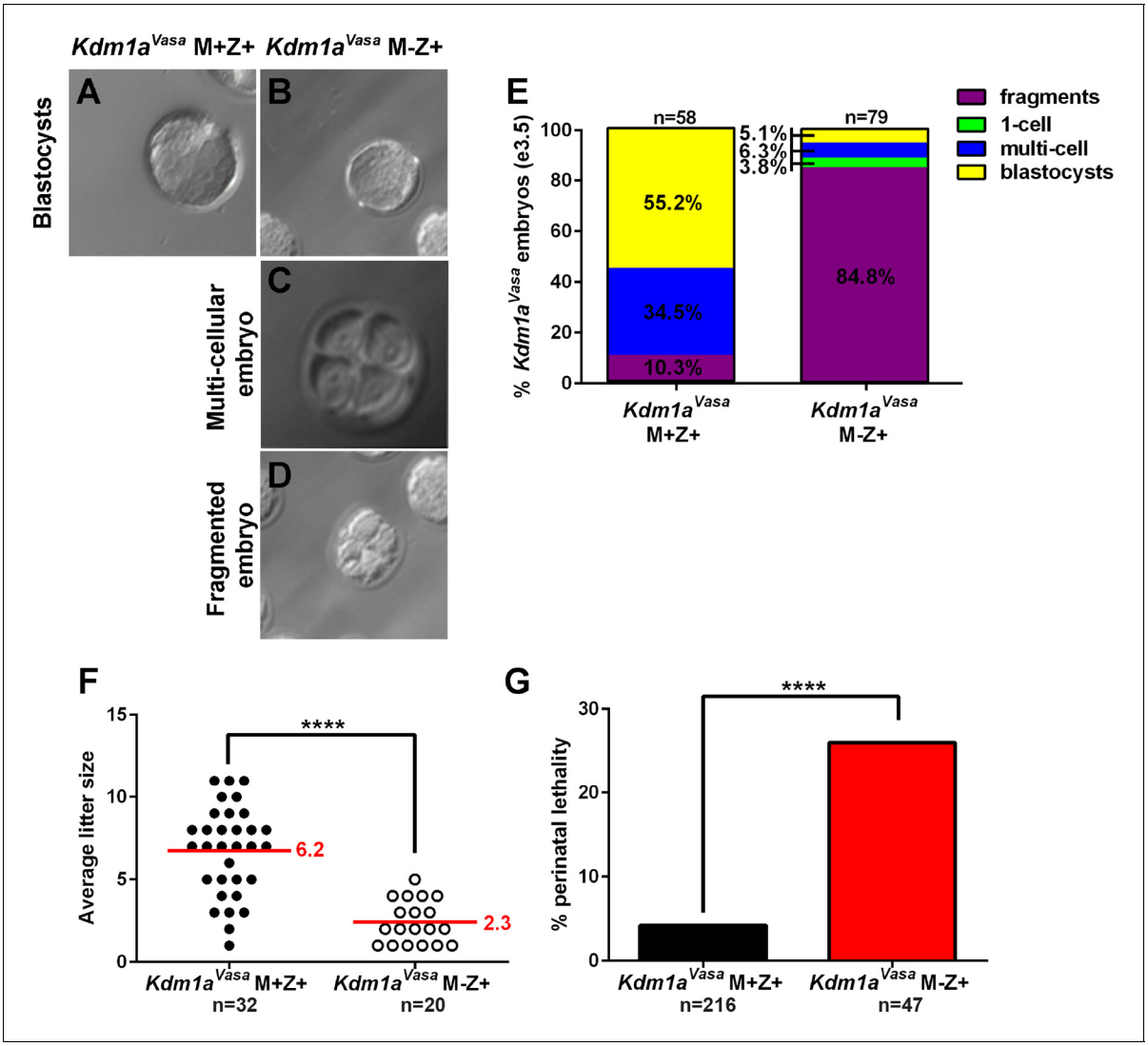

Figure 4. Hypomorphic phenotype in *Kdm1a*^{Vasa} progeny. (**A–D**) Brightfield images of M+Z+. (**A**) and M-Z+ (**B–D**) embryos derived from *Kdm1a*^{Vasa} control and mutant mothers at embryonic day 3.5 (e3.5). Panels show blastocysts (**A**,**B**), a multicellular embryo (**C**) and a fragmented embryo (**D**). (**E**) Percentage of fragmented (purple), 1-cell (green), multi-cellular (blue) and blastocyst (yellow) embryos from *Kdm1a*^{Vasa} control and mutant mothers at e3.5. n = 58 for *Kdm1a*^{Vasa} M+Z+ embryos from 7 litters. n = 79 for *Kdm1a*^{Vasa} M-Z+ embryos from 10 litters. (**F**) Litter sizes of *Kdm1a*^{Vasa} control and mutant mothers. Average litter size for each indicated by red line. Each circle indicates one litter and n=number of litters analyzed. p-values calculated using an unpaired t-test with **** = p<0.0001 indicating statistical significance. (**G**) Percentage of newborn pups from *Kdm1a*^{Vasa} heterozygous control and mutant mothers that died perinatally. n = number of litters analyzed. p-values calculated using an unpaired t-test with **** = p<0.0001 indicating statistical significance.

DOI: 10.7554/eLife.08848.018

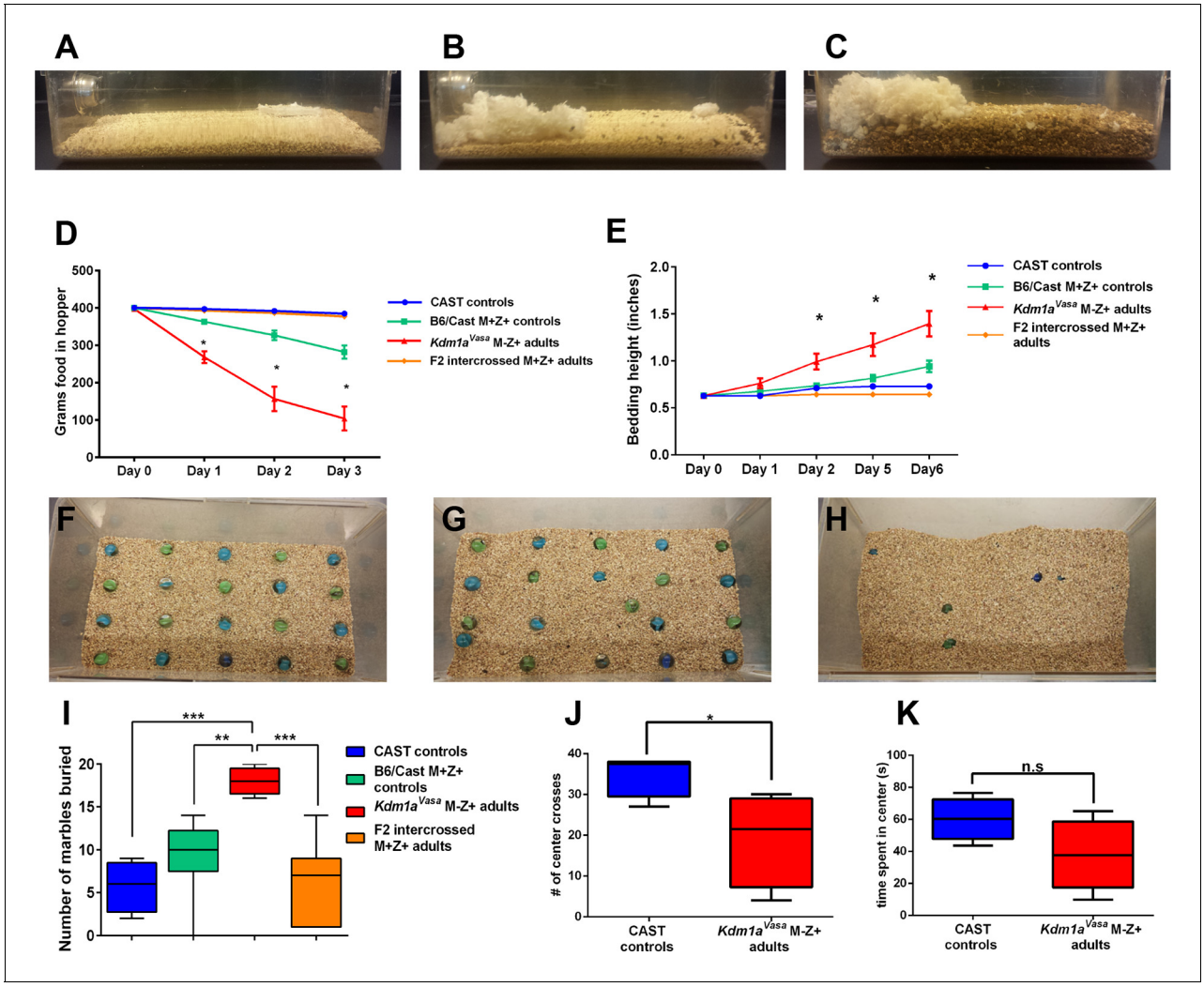

Figure 5. Abnormal behaviors in *Kdm1a*^{Vasa} M-Z+ adults. (**A–C**) Mouse cages at day 0 (**A**) and day 8 (**B**) from *M. castaneus* (CAST) controls compared to day 6 (**C**) from a *Kdm1a*^{Vasa} M-Z+ adult. (**D**) Quantification of change in weight of food in the hopper from CAST controls, B6/CAST hybrid M+Z+ controls, and F2 intercrossed M+Z+ adults versus *Kdm1a*^{Vasa} M-Z+ adults. Data are shown as mean for each day with error bars indicating ± S.E.M. (**E**) Quantification of change in bedding height from CAST controls, B6/CAST hybrid M+Z+ controls, and F2 intercrossed M+Z+ adults versus *Kdm1a*^{Vasa} M-Z+ adults. Data are shown as mean for each day with error bars indicating ± S.E.M. (**F–H**) Mouse cages before (**F**) and after (**G**,**H**) the marble burying assay was performed on a CAST control (**G**) compared to a *Kdm1a*^{Vasa} M-Z+ adult (**H**). (**I**) Quantification of the number of marbles buried during the marble burying assay performed on CAST controls, B6/CAST hybrid M+Z+ controls, and F2 intercrossed M+Z+ adults versus *Kdm1a*^{Vasa} M-Z+ adults. Data are shown as quartiles with error bars indicating ± S.E.M. (**J**,**K**) Open field test performance in CAST controls versus *Kdm1a*^{Vasa} M-Z+ adults scored by number of center crosses (**J**) and time spent in center of cage (**K**). Data are shown as quartiles with error bars indicating ± S.E.M. p-values calculated using an unpaired t-test with n.s. indicating p>0.05, * = p<0.05, ** = p<0.005, *** = p<0.0005. All asterisks indicate statistical significance.
DOI: 10.7554/eLife.08848.020

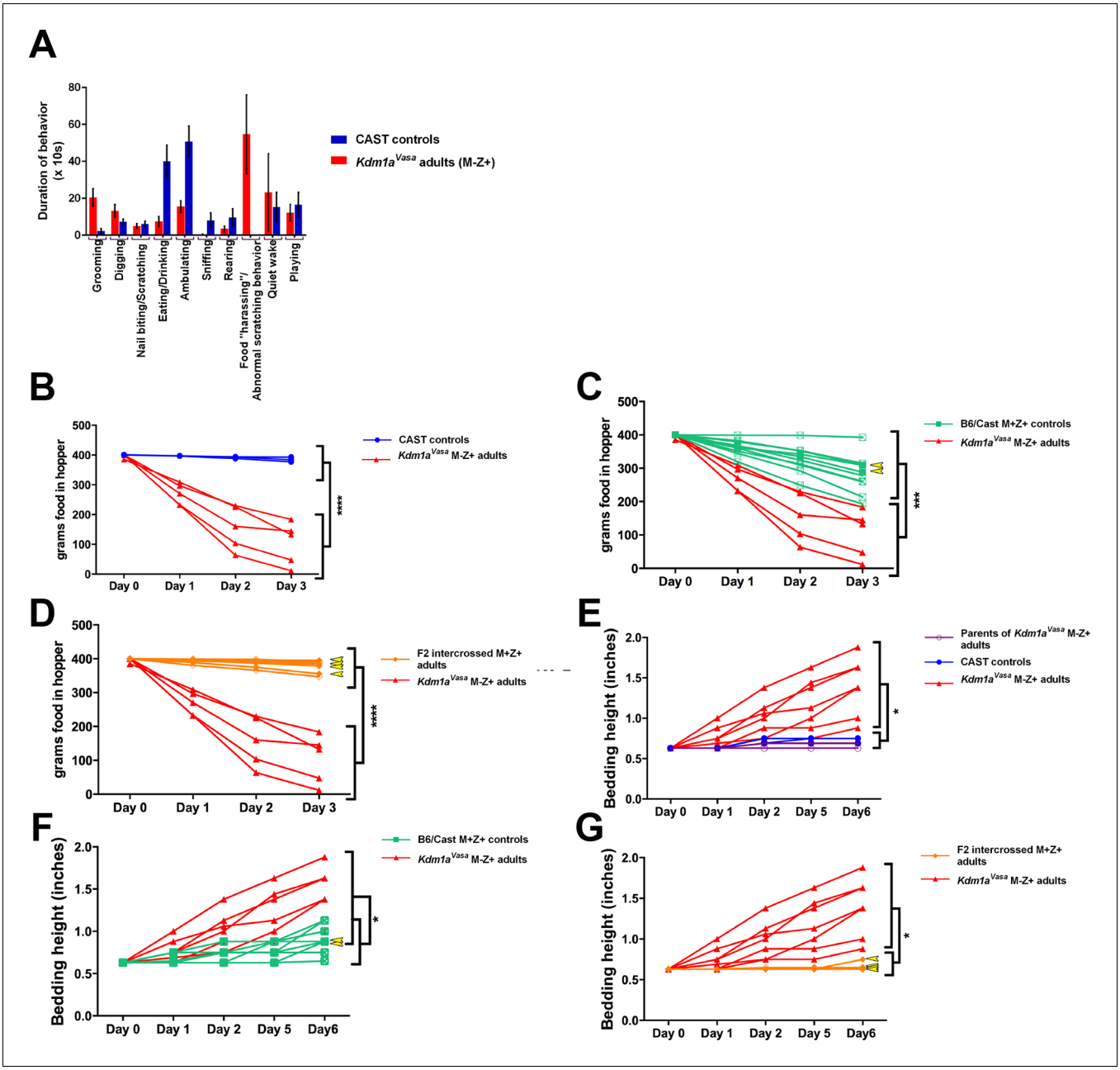

Figure 5—figure supplement 1. Abnormal behaviors in individual *Kdm1a*^{Vasa} M-Z+ adults. (**A**) Behavioral ethogram of *M. castaneus* (CAST) controls versus *Kdm1a*^{Vasa} M-Z+ adults. (**B**) Quantification of change in weight of food in the hopper of parents of *Kdm1a*^{Vasa} M-Z+ adults and CAST controls versus *Kdm1a*^{Vasa} M-Z+ adults. (**C**) Quantification of change in weight of food in the hopper of B6/CAST M+Z+ controls versus *Kdm1a*^{Vasa} M-Z+ adults. (**D**) Quantification of change in weight of food in the hopper of F2 intercrossed M+Z+ adults versus *Kdm1a*^{Vasa} M-Z+ adults. (**E**) Quantification of change in bedding height of parents of *Kdm1a*^{Vasa} M-Z+ adults and CAST controls versus *Kdm1a*^{Vasa} M-Z+ adults. (**F**) Quantification of change in bedding height of B6/CAST M+Z+ controls versus *Kdm1a*^{Vasa} M-Z+ adults. (**G**) Quantification of change in bedding height of F2 intercrossed M+Z+ adults versus *Kdm1a*^{Vasa} M-Z+ adults. The measurements for each individual animal (**B–D**) and (**E–G**) correspond to the averages shown in ***Figure 5 (D, E***). Yellow arrowheads represent animals heterozygous for *Kdm1a*. Data shown as mean for each day. p-values calculated using an unpaired t-test with * = p<0.05, *** = p<0.0005, **** = p<0.0001. All asterisks indicate statistical significance.

DOI: 10.7554/eLife.08848.021

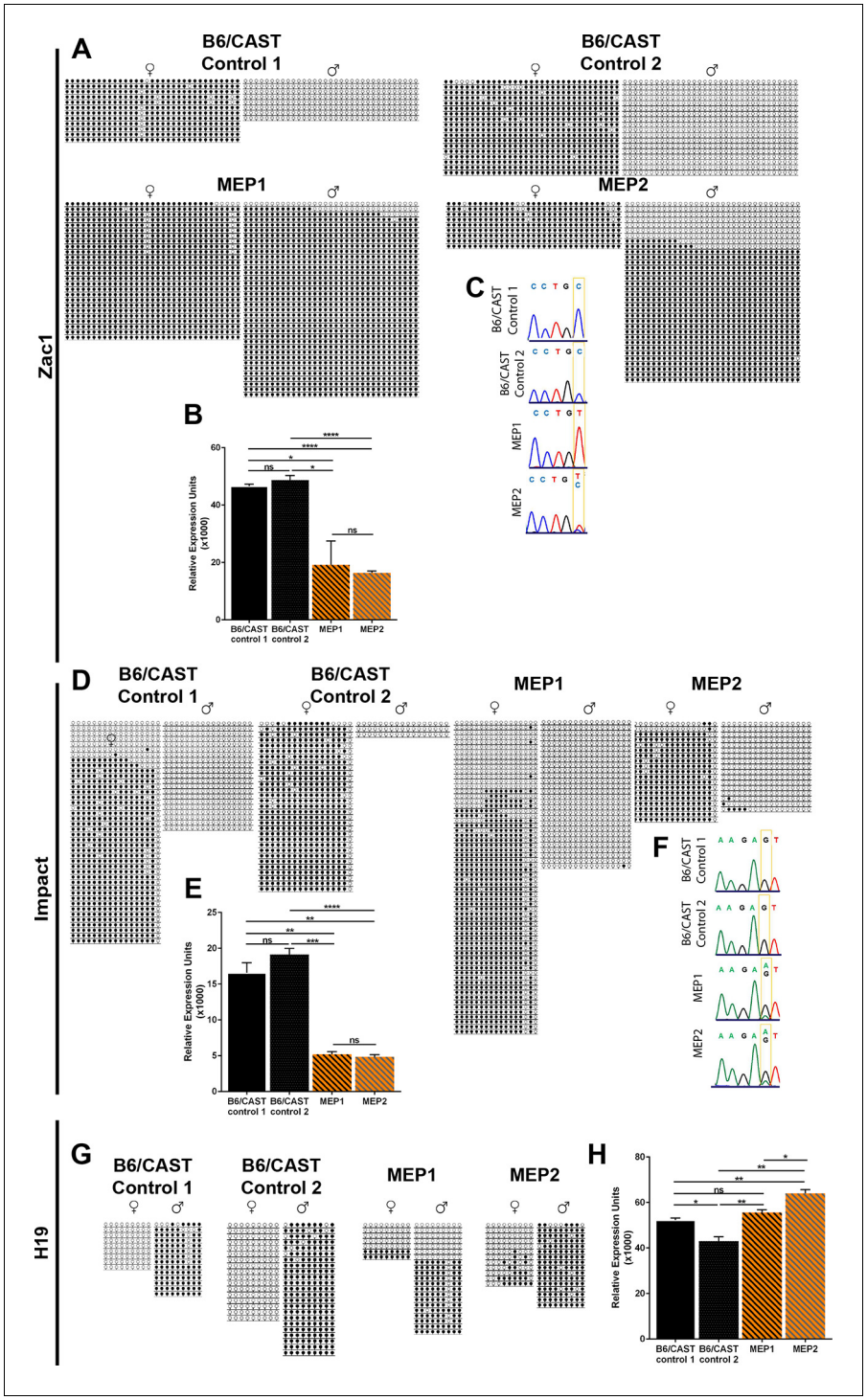

Figure 6. Imprinting defects in *Kdm1a*^{Vasa} progeny. (**A**,**D**,**G**) Allele-specific bisulfite analysis of *Zac1* (**A**), *Impact* (**D**), and *H19* (**G**). Each line represents the clone of an allele. Each circle represents a CpG dinucleotide where closed circles indicate methylation and open circles indicate no methylation. Maternal and paternal alleles are indicated. (**B**,**E**,**H**) Relative expression analysis of *Zac1* (**B**), *Impact* (**E**), and *H19* (**H**). Expression normalized to *β-actin*. Error bars indicate S.E.M. p-values calculated using an unpaired t-test with n.s. indicating p>0.05, * = p<0.05, ** = p<0.005, **** = p<0.0001. All asterisks indicate statistical significance. (**C**,**F**) Allele-specific expression of *Zac1* (**C**) and *Impact* (**F**). The polymorphic base is highlighted in yellow. For *Zac1*, the maternal allele SNP is T (red) in highlighted position and paternal allele SNP is C (blue) in electrophoretogram. For *Impact*, the maternal allele SNP is A (green) in highlighted position and paternal allele SNP is G (black) in electrophoretogram. All analyses

Figure 6 continued on next page

Figure 6 continued

were performed on 2 staged matched B6/CAST hybrid control pups and 2 maternal effect progeny (MEP) exhibiting perinatal lethality.

DOI: 10.7554/eLife.08848.024

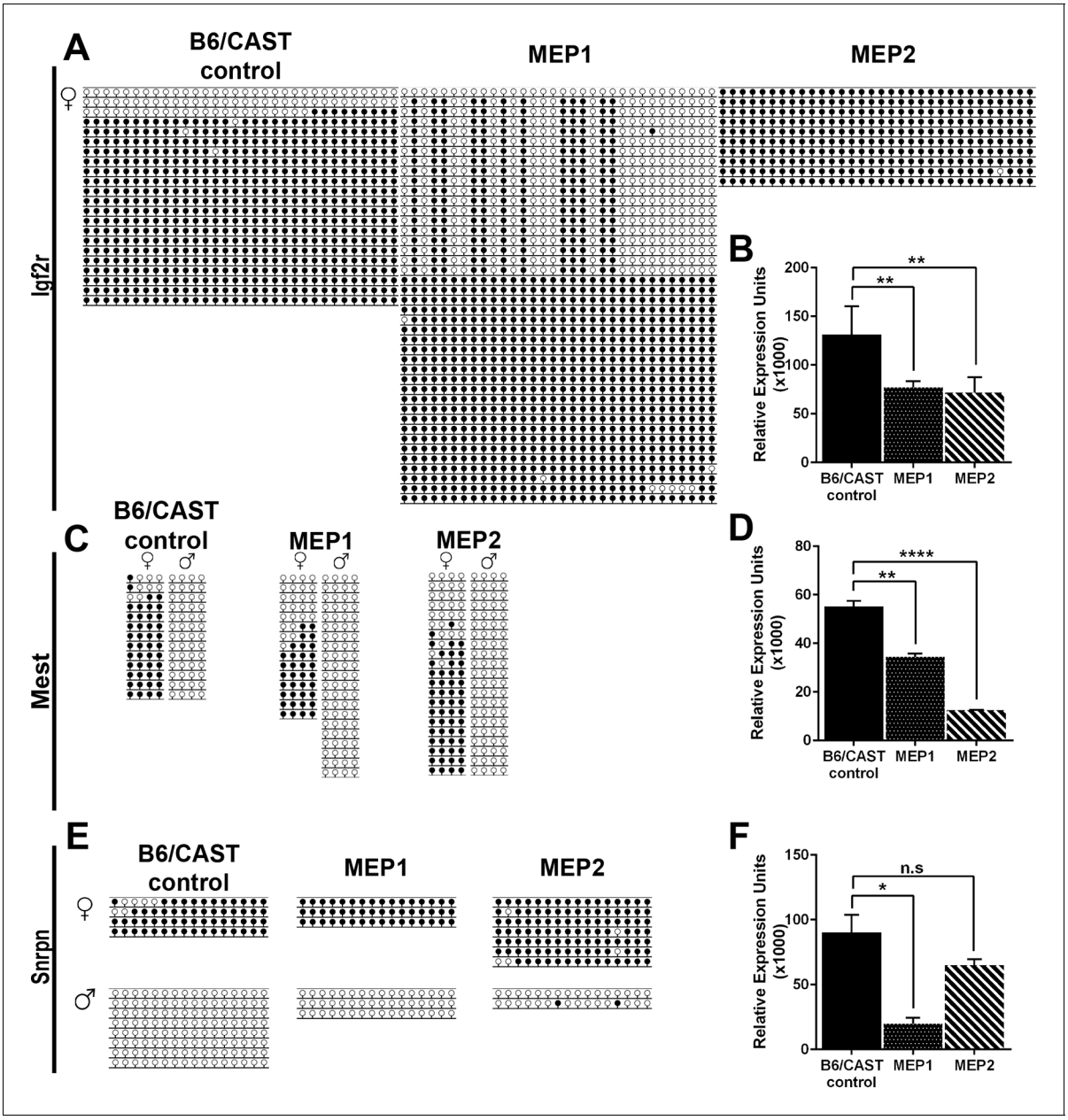

Figure 6—figure supplement 1. Imprinting analysis of *Kdm1a*^{Vasa} progeny. (**A**,**C**,**E**) Allele-specific bisulfite analysis of, *Igf2r* (**A**), *Mest* (**C**), and *Snrpn* (**E**). Each line represents the clone of an allele. Each circle represents a CpG dinucleotide where closed circles indicate methylation and open circles indicate no methylation. Maternal and paternal alleles are indicated. (**B**,**D**,**F**) Relative expression analysis of *Igf2r* (**B**), *Mest* (**D**), and *Snrpn* (**F**). Expression normalized to *β-actin*. Error bars indicate ± S.E.M. p-values calculated using an unpaired t-test with n.s. indicating p>0.05, * = p<0.05, ** = p<0.005, **** = p<0.0001. All asterisks indicate statistical significance. All analyses were performed on a stage matched B6/CAST hybrid control pup and 2 maternal effect progeny (MEP) exhibiting perinatal lethality.

DOI: 10.7554/eLife.08848.025

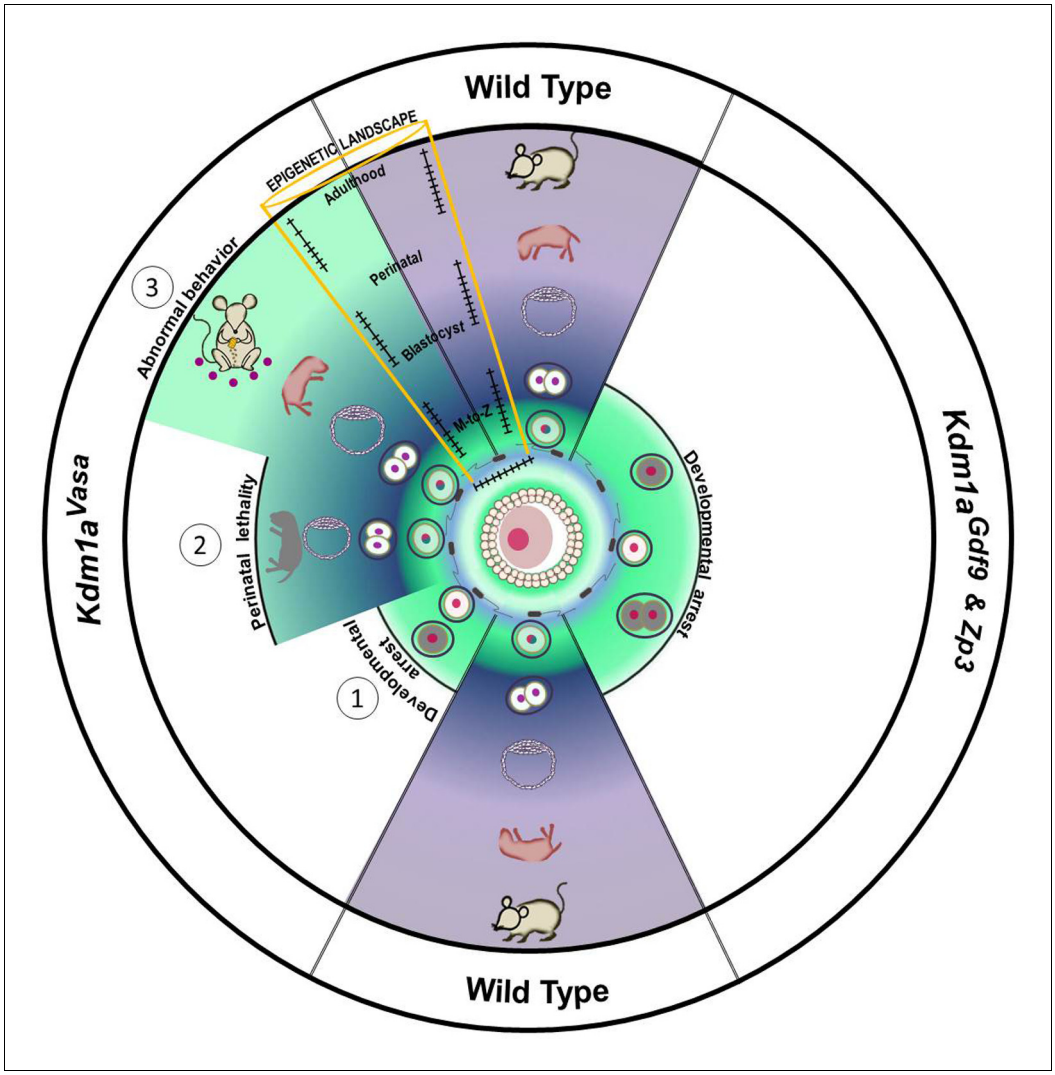

Figure 7. Model. Loss of maternal LSD1 results in defects later in development in wild-type oocytes, after fertilization (denoted by blue sperm encircling oocyte) the fertilized egg undergoes the maternal to zygotic transition (MZT; green to blue/purple) at the 1–2 cell stage. These M+Z+ embryos proceed normally through development (indicated by blastocyst, perinatal stage pup, and adult mouse). In contrast, when Lsd1 is deleted with either Gdf9- or Zp3-Cre, the resulting Lsd1Gdf9 and Lsd1Zp3 progeny become arrest at the 1–2 cell stage and never undergo the MZT (green). When Lsd1 is deleted with Vasa-Cre, we observe 3 hypomorphic outcomes in resulting Lsd1Vasa progeny: (1) developmental arrest at the 1–2 cell stage, (2) perinatal lethality and (3) abnormal behavior in surviving adult animals. These outcomes are due to reduced LSD1 in the mothers oocyte, suggesting that lowered maternal LSD1 can result in defects much later in development. These long-range outcomes are associated with imprinting defects (depicted as wild-type versus mutant changes in DNA methylation within the yellow region).

DOI: 10.7554/eLife.08848.027